CHAPTER 2

Numerical stability and dispersion

2.1 Numerical stability

The finite-difference time-domain (FDTD) algorithm samples the electric and magnetic fields at discrete points both in time and space. The choice of the period of sampling (Δt in time, Δx, Δy, and Δz in space) must comply with certain restrictions to guarantee the stability of the solution. Furthermore, the choice of these parameters determines the accuracy of the solution. This section focuses on the stability analysis. First, the stability concept is illustrated using a simple partial differential equation (PDE) in space and time domain. Next, the Courant-Friedrichs-Lewy (CFL) condition [3] for the FDTD method is discussed, accompanied by a one-dimensional FDTD example.

2.1.1 Stability in time-domain algorithm

An important issue in designing a time-domain numerical algorithm is the stability condition. To understand the stability concept, let's start with a simple wave equation:

$$\frac{\partial u(x,t)}{\partial t} + \frac{\partial u(x,t)}{\partial x} = 0, \quad u(x, t=0) = u_0(x), \tag{2.1}$$

where $u(x, t)$ is the unknown wave function and $u_0(x)$ is the initial condition at $t = 0$. Using the PDE knowledge, the equation can be analytically solved:

$$u(x,t) = u_0(x - t). \tag{2.2}$$

A time-domain numerical scheme can be developed to solve above wave equation. First, $u(x, t)$ is discretized in both time and space domains:

$$\begin{aligned} x_i &= i\Delta x, \quad i = 0, 1, 2, \ldots \\ t_n &= n\Delta t, \quad n = 0, 1, 2, \ldots \\ u_i^n &= u(x_i, t_n). \end{aligned} \tag{2.3}$$

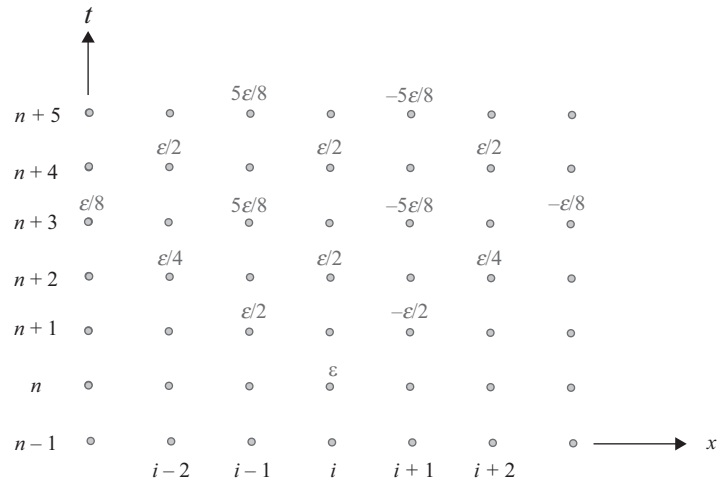

Figure 2.1 The time–space domain grid with error ε propagating with $\lambda = 1/2$.

Here, Δt and Δx are the time and space cell sizes. Then, the finite-difference scheme is used to compute the derivatives, and the following equation is obtained:

$$\frac{u_i^{n+1} - u_i^{n-1}}{2\Delta t} + \frac{u_{i-1}^{n} - u_{i+1}^{n}}{2\Delta x} = 0. \tag{2.4}$$

After a simple manipulation, a time-domain numerical scheme can be derived such that

$$u_i^{n+1} = u_i^{n-1} + \lambda(u_{i+1}^{n} - u_{i-1}^{n}), \quad \lambda = \frac{\Delta t}{\Delta x}. \tag{2.5}$$

Figure 2.1 shows a time and space domain grid, where the horizontal axis represents the x axis and the vertical axis denotes the t axis. The u values for time index denoted as n and $n - 1$ are all assumed to be known. For simplicity we will assume that all these values are zeros. We will also assume that at one x position denoted by the index i and at time denoted by the index n there is a small error represented by the parameter ε. As the time evolves, a u value at $n + 1$ is computed from two rows lower in accordance with (2.5).

Now let's analyze the propagation of the assumed numerical error ε in this time-domain algorithm. Note that the error may result from a numerical truncation of a real number. When $\lambda = 1/2$, the errors are shown in Figure 2.1. The error will keep propagating in this time-domain algorithm; however, it can be observed that the errors are always bounded by the original error ε, whereas for the case when $\lambda = 1$, the maximum absolute value of the propagating error is of the same value as the original error. This is clearly obvious from the errors propagating in Figure 2.2. On the contrary, when $\lambda = 2$, the propagation of error as shown in Figure 2.3 will keep increasing as time evolves. Finally, this error will be large enough and will destroy the actual u values. As a result, the time-domain algorithm will not give an accurate result due to a very small initial error. In summary, the numerical scheme in (2.5) is therefore considered conditionally stable. It is stable for small λ values but unstable for large λ values, and the boundary of stability condition is $\lambda = 1$.

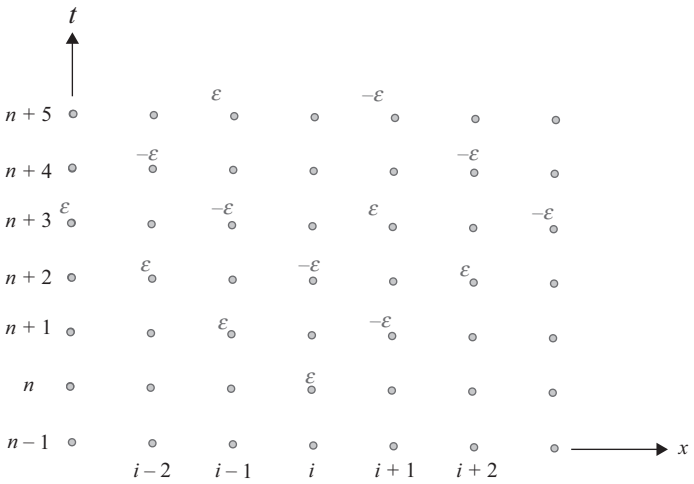

Figure 2.2 The time–space domain grid with error ε propagating with $\lambda = 1$.

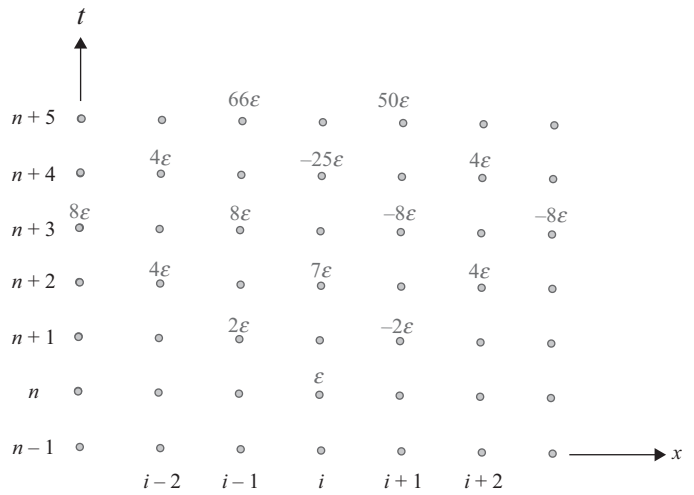

Figure 2.3 The time–space domain grid with error ε propagating with $\lambda = 2$.

2.1.2 CFL condition for the FDTD method

The numerical stability of the FDTD method is determined by the CFL condition, which requires that the time increment Δt has a specific bound relative to the lattice space increments, such that

$$\Delta t \leq \frac{1}{c\sqrt{\frac{1}{(\Delta x)^2} + \frac{1}{(\Delta y)^2} + \frac{1}{(\Delta z)^2}}}, \tag{2.6}$$

where c is the speed of light in free space. Equation (2.6) can be rewritten as

$$c\Delta t\sqrt{\frac{1}{(\Delta x)^2}+\frac{1}{(\Delta y)^2}+\frac{1}{(\Delta z)^2}}\leq 1. \tag{2.7}$$

For a cubical spatial grid where $\Delta x = \Delta y = \Delta z$, the CFL condition reduces to

$$\Delta t \leq \frac{\Delta x}{c\sqrt{3}}. \tag{2.8}$$

One can notice in (2.6) that the smallest value among Δx, Δy, and Δz is the dominant factor controlling the maximum time step and that the maximum time step allowed is always smaller than $\min(\Delta x, \Delta y, \Delta z)/c$.

In the one-dimensional case where $\Delta y \to \infty$ and $\Delta z \to \infty$ in (2.6), the CFL condition reduces to

$$\Delta t \leq \Delta x/c \quad \text{or} \quad c\Delta t \leq \Delta x. \tag{2.9}$$

This equation implies that a wave cannot be allowed to travel more than one cell size in space during one time step.

The existence of instability exposes itself as the development of divergent spurious fields in the problem space as the FDTD iterations proceed. For instance, the one-dimensional FDTD code presented in Chapter 1 simulates a problem space composed of cells having length $\Delta x = 1$ mm. Due to the one-dimensional CFL condition (2.9) the time increment must be chosen as $\Delta t \leq 3.3356$ ps. This code is run with the values of $\Delta t = 3.3356$ ps and $\Delta t = 3.3357$ ps, and the maximum value of electric field magnitude is captured at every time step and plotted in Figure 2.4. The spikes of the electric field magnitude are due to the

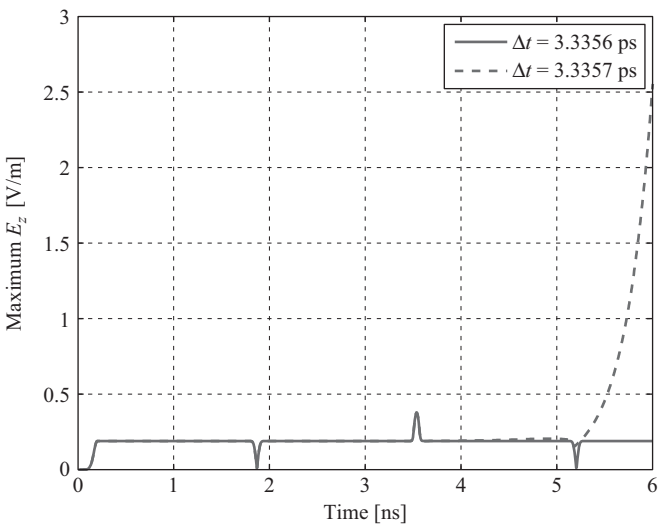

Figure 2.4 Maximum magnitude of E_z in the one-dimensional problem space for simulations with $\Delta t = 3.3356$ ps and $\Delta t = 3.3357$ ps.

additive interference of the fields when fields pass through the center of the problem space, and the nulls are due to the vanishing of electric fields on PEC when the fields hit the PEC boundary walls. However, while the iterations proceed, the electric field magnitude calculated by the simulation running with $\Delta t = 3.3357$ ps starts to diverge. This examination demonstrates how a Δt value larger than the CFL limit gives rise to instability in the FDTD computation.

The CFL stability condition applies to inhomogeneous media as well, since the velocity of propagation in material media is smaller than c. However, numerical stability can be influenced by other factors, such as absorbing boundary conditions, nonuniform spatial grids, and nonlinear materials.

Even if the numerical solution is stable, satisfaction of the CFL condition does not guarantee the numerical accuracy of the solution; it only provides a relationship between the spatial grid size and the time step. One must still satisfy the sampling theory requirements with respect to the highest frequency present in the excitation.

2.2 Numerical dispersion

The FDTD method provides a solution for the behavior of fields that is usually a good approximation to the real physical behavior of the fields. The finite-difference approximation of derivatives of continuous functions introduces an error to the solution. For instance, even in homogeneous free space, the velocity of propagation of the numerical solution for a wave will generally differ from c. Furthermore, it will vary with frequency, the spatial grid size, and direction of propagation of the wave. The differing of phase velocities numerically obtained by the FDTD method from the actual phase velocities is known as numerical dispersion.

For instance, consider a plane wave propagating in free space in the x direction, given by

$$E_z(x,t) = E_0 \cos(k_x x - \omega t), \tag{2.10a}$$

$$H_y(x,t) = H_0 \cos(k_x x - \omega t). \tag{2.10b}$$

Here, $E_z(x, t)$ satisfies the wave equation

$$\frac{\partial^2}{\partial x^2} E_z - \mu_0 \varepsilon_0 \frac{\partial^2}{\partial t^2} E_z = 0. \tag{2.11}$$

Substituting (2.10a) in (2.11) yields the equation

$$k_x^2 = \omega^2 \mu_0 \varepsilon_0 = \left(\frac{\omega}{c}\right)^2, \tag{2.12}$$

which is called the *dispersion relation*. The dispersion relation provides the connection between the spatial frequency k_x and the temporal frequency ω [4]. The dispersion relation (2.12) is analytically exact.

A dispersion relation equation, which is called the numerical dispersion relation, can be obtained based on the finite-difference approximation of Maxwell's curl equations as follows. For the one-dimensional case previously discussed, the plane wave expressions

$E_z(x, t)$ and $H_y(x, t)$ satisfy the Maxwell's one-dimensional curl equations, which are given for the source-free region as

$$\frac{\partial E_z}{\partial t} = \frac{1}{\varepsilon_0}\frac{\partial H_y}{\partial x}, \tag{2.13a}$$

$$\frac{\partial H_y}{\partial t} = \frac{1}{\mu_0}\frac{\partial E_z}{\partial x}. \tag{2.13b}$$

These equations can be rewritten using the central difference formula based on the field positioning scheme in Figure 1.13 as

$$\frac{E_z^{n+1}(i) - E_z^n(i)}{\Delta t} = \frac{1}{\varepsilon_0}\frac{H_y^{n+\frac{1}{2}}(i) - H_y^{n+\frac{1}{2}}(i-1)}{\Delta x}, \tag{2.14a}$$

$$\frac{H_y^{n+\frac{1}{2}}(i) - H_y^{n-\frac{1}{2}}(i)}{\Delta t} = \frac{1}{\mu_0}\frac{E_z^n(i+1) - E_z^n(i)}{\Delta x}. \tag{2.14b}$$

The plane wave equations (2.10) are in continuous time and space, and they can be expressed in discrete time and space with

$$E_z^n(i) = E_0\cos(k_x i\Delta x - \omega n\Delta t), \tag{2.15a}$$

$$E_z^{n+1}(i) = E_0\cos(k_x i\Delta x - \omega(n+1)\Delta t), \tag{2.15b}$$

$$E_z^n(i+1) = E_0\cos(k_x(i+1)\Delta x - \omega n\Delta t), \tag{2.15c}$$

$$H_y^{n+\frac{1}{2}}(i) = H_0\cos(k_x(i+0.5)\Delta x - \omega(n+0.5)\Delta t), \tag{2.15d}$$

$$H_y^{n+\frac{1}{2}}(i-1) = H_0\cos(k_x(i-0.5)\Delta x - \omega(n+0.5)\Delta t), \tag{2.15e}$$

$$H_y^{n-\frac{1}{2}}(i) = H_0\cos(k_x(i+0.5)\Delta x - \omega(n-0.5)\Delta t), \tag{2.15f}$$

The terms (2.15a), (2.15b), (2.15d), and (2.15e) can be used in (2.14a) to obtain

$$\frac{E_0}{\Delta t}\Big[\cos(k_x i\Delta x - \omega(n+1)\Delta t) - \cos(k_x i\Delta x - \omega n\Delta t)\Big]$$
$$= \frac{H_0}{\varepsilon_0\Delta x}\Big[\cos(k_x(i+0.5)\Delta x - \omega(n+0.5)\Delta t) - \cos(k_x(i-0.5)\Delta x - \omega(n+0.5)\Delta t)\Big]. \tag{2.16}$$

Using the trigonometric identity

$$\cos(u-v) - \cos(u+v) = 2\sin(u)\sin(v)$$

on the left-hand side of (22.16) with $u = k_x i\Delta x - \omega(n + 0.5)\Delta t$ and $v = 0.5\Delta t$, and on the right-hand side with $u = k_x i\Delta x - \omega(n + 0.5)\Delta t$ and $v = -0.5\ \Delta x$, one can obtain

$$\frac{E_0}{\Delta t}\sin(0.5\omega\Delta t) = \frac{-H_0}{\varepsilon_0\Delta x}\sin(0.5k_x\Delta x). \tag{2.17}$$

Similarly, using the terms (2.15a), (2.15c), (2.15d), and (2.15f) in (2.14b) leads to

$$\frac{H_0}{\Delta t}\sin(0.5\omega\Delta t) = \frac{-E_0}{\mu_0 \Delta x}\sin(0.5k_x\Delta x). \tag{2.18}$$

Combining (2.17) and (2.18) one can obtain the numerical dispersion relation for the one-dimensional case as

$$\left[\frac{1}{c\Delta t}\sin\left(\frac{\omega\Delta t}{2}\right)\right]^2 = \left[\frac{1}{\Delta x}\sin\left(\frac{k_x\Delta x}{2}\right)\right]^2. \tag{2.19}$$

One should notice that the numerical dispersion relation (2.19) is different from the ideal dispersion relation (2.12). The difference means that there is a deviation from the actual solution of a problem and, hence, an error introduced by the finite-difference approximations to the numerical solution of the problem. However, it is interesting to note that for the one-dimensional case, if one sets $\Delta t = \Delta x/c$ (2.19) reduces to (2.12), which means that there is no dispersion error for propagation in free space. However, this is of little practical use, since the introduction of a material medium will again create dispersion.

So far, derivation of a numerical dispersion relation has been demonstrated for a one-dimensional case. It is possible to obtain a numerical dispersion relation for the two-dimensional case using a similar approach:

$$\left[\frac{1}{c\Delta t}\sin\left(\frac{\omega\Delta t}{2}\right)\right]^2 = \left[\frac{1}{\Delta x}\sin\left(\frac{k_x\Delta x}{2}\right)\right]^2 + \left[\frac{1}{\Delta y}\sin\left(\frac{k_y\Delta y}{2}\right)\right]^2, \tag{2.20}$$

where there is no variation of fields or geometry in the z dimension. For the particular case where

$$\Delta x = \Delta y = \Delta, \quad \Delta t = \frac{\Delta}{c\sqrt{2}}, \quad \text{and} \quad k_x = k_y,$$

the ideal dispersion relation for the two-dimensional case can be recovered as

$$k_x^2 + k_y^2 = \left(\frac{\omega}{c}\right)^2. \tag{2.21}$$

The extension to the three-dimensional case is straightforward but tedious, yielding

$$\left[\frac{1}{c\Delta t}\sin\left(\frac{\omega\Delta t}{2}\right)\right]^2 = \left[\frac{1}{\Delta x}\sin\left(\frac{k_x\Delta x}{2}\right)\right]^2 + \left[\frac{1}{\Delta y}\sin\left(\frac{k_y\Delta y}{2}\right)\right]^2 + \left[\frac{1}{\Delta z}\sin\left(\frac{k_z\Delta z}{2}\right)\right]^2. \tag{2.22}$$

Similar to the one- and two-dimensional cases, it is possible to recover the three-dimensional ideal dispersion relation

$$k_x^2 + k_y^2 + k_z^2 = \left(\frac{\omega}{c}\right)^2 \tag{2.23}$$

for specific choices of Δt, Δx, Δy, Δz, and angle of propagation.

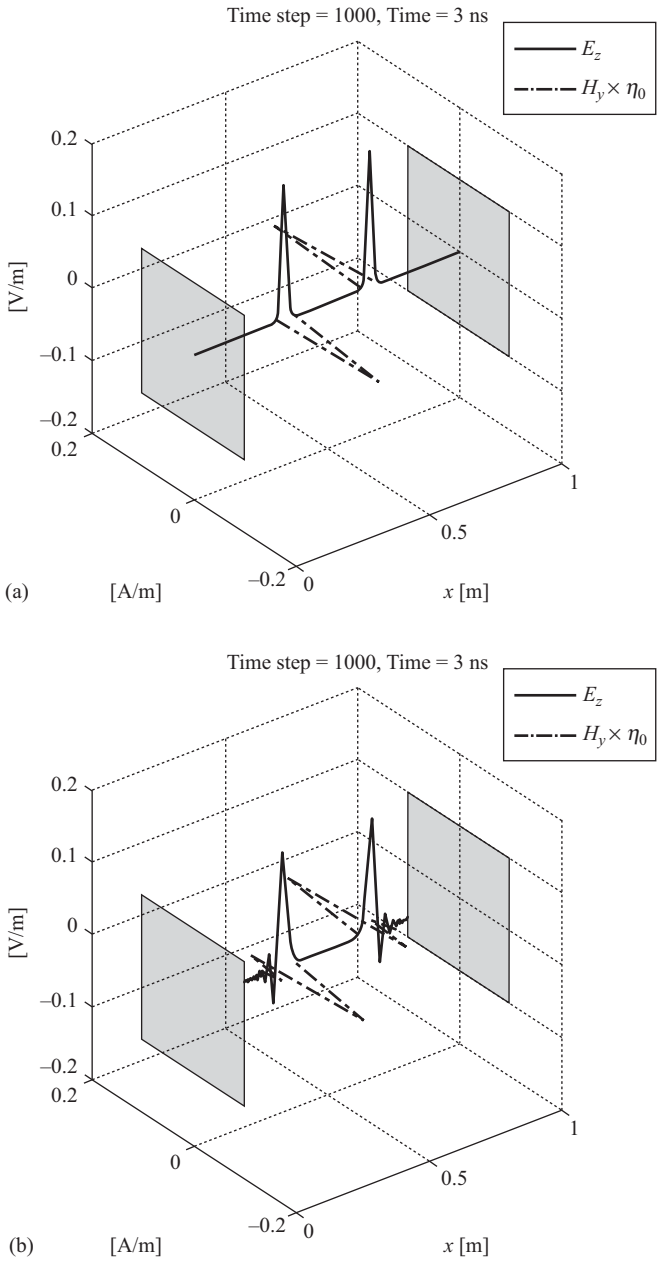

Figure 2.5 (a) Maximum magnitude of E_z in the one-dimensional problem space: simulation with $\Delta x = 1$ mm; (b) maximum magnitude of E_z in the one-dimensional problem space: simulation with $\Delta x = 4$ mm.

Let's rewrite (2.22) in the following form:

$$\left[\frac{\omega}{2c}\frac{\sin(\omega\Delta t/2)}{(\omega\Delta t/2)}\right]^2 = \left[\frac{k_x}{2}\frac{\sin(k_x\Delta x/2)}{(k_x\Delta x/2)}\right]^2 + \left[\frac{k_y}{2}\frac{\sin(k_y\Delta y/2)}{(k_y\Delta y/2)}\right]^2 + \left[\frac{k_z}{2}\frac{\sin(k_z\Delta z/2)}{(k_z\Delta z/2)}\right]^2. \quad (2.24)$$

Since $\lim_{x\to 0}(\sin(x)/x) = 1$ (2.24) reduces to the ideal dispersion relation (2.23) when $\Delta t \to 0$, $\Delta x \to 0$, $\Delta y \to 0$, and $\Delta z \to 0$. This is an expected result since when the sampling periods approach zero, the discrete approximation turns into the continuous case. This also indicates that if the temporal and spatial sampling periods Δt, Δx, Δy, and Δz are taken smaller, then the numerical dispersion error reduces.

So far, we have discussed the numerical dispersion in the context of waves propagating in free space. A more general discussion of numerical stability and dispersion, including the derivation of two- and three-dimensional numerical dispersion relations, other factors affecting the numerical dispersion, and strategies to reduce the associated errors, can be found in [1]. We conclude our discussion with an example demonstrating the numerical dispersion.

Due to numerical dispersion, waves with different frequencies propagate with different phase velocities. Any waveform is a sum of sinusoidal waves with different frequencies, and a waveform does not maintain its shape while propagating since its sinusoidal components do not propagate with the same velocity due to dispersion. Therefore, the existence of numerical dispersion exposes itself as distortion of the waveform. For instance, Figure 2.5 shows the electric and magnetic field in the one-dimensional problem space calculated by the one-dimensional FDTD code presented in Chapter 1. The problem space is 1 m wide, and $\Delta t = 3$ ps. Figure 2.5(a) shows the field distribution at time instant 3 ns as calculated by the program when $\Delta x = 1$ mm and $J_z = 1$ A/m^2. Similarly, Figure 2.5(b) shows the field distribution at time instant 3 ns when $\Delta x = 4$ mm. In this second simulation the magnitude of J_z is taken as 0.25 A/m^2 to maintain the magnitude of the surface current density K_z as 1×10^{-3} A/m; hence, the magnitudes of electric and magnetic fields are almost the same. Figure 2.5(a) shows that the Gaussian pulse is not distorted; even though there is numerical dispersion, it is not significant. However, in Figure 2.5(b) the Gaussian pulse is distorted due to use of a larger cell size, and the error introduced by numerical dispersion is more pronounced.

2.3 Exercises

2.1 Using the one-dimensional MATLAB® FDTD program listed in Appendix A, verify the results presented in Figure 2.5.

2.2 Update the one-dimensional FDTD MATLAB program such that the Gaussian pulse propagates in a medium characterized with electric losses instead of free space. Observe the decay of the amplitude of the propagating pulse and the effect of losses on the dispersion shown in Figure 2.5(b) at time = 3 ns.

2.3 Repeat Exercise 2.2, but with the introduction of magnetic losses in the medium, instead of free space. Record your observations related to the pulse propagation at time = 3 ns.